Songklanakarin J. Sci. Technol.
41 (3), 494-500, May – Jun. 2019

http://www.sjst.psu.ac.th

Original Article

Development of high-temperature multi-magnetron microwave furnace for material processing

Direk Boonthum[1], Singkarn Chanprateep[2], Chesta Ruttanapun[2], and Mudtorlep Nisoa[1*]

[1] *School of Science, Walailak University, Tha Sala, Nakhon Si Thammarat, 80160 Thailand*

[2] *Department of Physics, Faculty of Science, King Mongkut's Institute of Technology Ladkrabang, Lat Krabang, Bangkok, 10520 Thailand*

Received: 4 May 2017; Revised: 7 November 2017; Accepted: 19 December 2017

Abstract

In this paper, we have successfully developed a multi-magnetron multi-mode high-temperature furnace for material processing. The SiC crucible could be heated to 1000 °C within only a few minutes. Synthesis of thermoelectric Al-doped ZnO in a microwave furnace took less than 20 times the time of a conventional furnace, and the electric power of Al-doped ZnO was higher. The furnace was fabricated according to the computational optimization using Comsol. Two waveguides were mounted on opposite sides of the cavity must have 90 degree relative angle. For impedance matching and power combination, the multi-mode rectangular cavity must have dimensions of 28 x 28 x 28 cm^3. Therefore, electric fields were maximized at the center of the cavity and minimized in the waveguides. To suppress the microwave leakage within safety standards, choke parameters were obtained. The calculations and measurements reinforce that scaling up can be done in the future.

Keywords: microwave furnace, multi-magnetrons, high temperature, processing of materials, Comsol Multi-physics

1. Introduction

Because of their high melting points, processing of glasses, metals and ceramics require high temperatures in hundreds or thousands of degree Celsius. Various heating technologies have been developed for high-temperature material processing. The technologies are classified as contact and non-contact methods. For the contact method, heat transfer to the materials is by hot air convection or infrared irradiation, resulting in direct heating of the materials. On the other hand, in the non-contact method, the heat sources produce microwave or radio frequency (RF) waves; the waves propagate into the materials which are then transformed into heat or thermal energy inside the materials. Such energy conversion is due to interactions between the materials and electromagnetic fields (Oghbaei & Mirzaee, 2010).

Microwaves are a form of electromagnetic waves with a frequency range between 300 MHz and 300 GHz (Bhattacharya & Basak, 2016). However, most processes in industrial and scientific activities use microwaves between 915 MHz and 2.45 GHz. The microwave propagation and heating of materials can be explained by Maxwell's equations. The interaction between microwaves and materials can be classified into three categories (Oghbaei & Mirzaee, 2010): (a) transparency; for low dielectric loss (ε_r'') materials, microwaves propagate through without any loss, (b) opaqueness; for conducting materials such as metals, microwaves are reflected at the surfaces and (c) absorption; for high dielectric loss materials, microwaves are absorbed and converted into heat. The amount of heating energy depends on the value of the dielectric loss. This mechanism of microwave heating is called

*Corresponding author
Email address: mnisoa@gmail.com

dielectric heating. The heating is effective for high dielectric loss materials (Mishra & Sharma, 2016). For low dielectric loss materials, such as ceramics, thermoelectric materials, dielectric heating is weak. Consequently, these materials are transparent to microwave energy.

In order to heat these materials, susceptors, good microwave absorbers, are used for preferential heating (Bhattacharya & Basak, 2016). This process is called indirect heating (Mishra & Sharma, 2016). Susceptors, such as silicon carbide (SiC) and molybdenum disilicide ($MoSi_2$), are highly lossy materials that can absorb microwave energy and convert it into heat very well (Panneerselvam, Agrawal, & Rao, 2003). The heat is transferred to the sample materials by irradiation. Because microwave processing of materials is a non-contact method and volumetric heating is not due to heat transfer by conduction or convection, microwave processing has many advantages over conventional methods (Oghbaei & Mirzaee, 2010). Microwave heating has very rapid heating rates that can hugely shorten processing times. The effectiveness of microwave heating saves electricity and cost. Mechanical and physical properties of the new materials and products are also improved. Processing of materials by microwave irradiation is a novel method used widely for heating a variety of materials. Microwave heating can achieve a wide range of temperatures which are suitable for various applications (Mishra & Sharma, 2016). These applications are classified according to temperature range into 3 groups: (1) low temperature processing of food, wood, rubber at T < 500 °C, (2) moderate temperature processing of metallic powders, carbon nanotubes (CNTs), ceramics, glass at 500 °C < T < 1000 °C and (3) high temperature processing of high-density ceramics, bulk metal joining, thermoelectric materials at T > 1000 °C (Mishra & Sharma, 2016).

Microwave heating technology has found many applications ranging from microwave ovens for cooking, to an apparatus for sterilization, and furnaces for materials processing. The microwave furnace for materials processing can have many shapes and forms. In general, there are two types, single mode and multi-mode cavity furnaces, depending on the resonant characteristics of the microwaves.

The advantage of the single mode furnace is its localized strong electric field that can easily heat materials to high temperature. However, there are several disadvantages, such as the difficulty in controlling the electric field intensity, the need for a stub tuner and circulator, the requirement for a high power magnetron. On the other hand, the multi-mode furnace has a high capacity cavity. The number of resonant modes is increased when the cavity size is larger (Mehrdad Mehdizadeh, 2015). Multi-mode furnaces that can generate temperatures higher than 1000 °C are already available in the market, however there are quite expensive. Many researchers have adapted microwave ovens for high temperature material processing at more than 1000 °C.

Since, microwave ovens are not designed for such high temperature usability, the high heat flux will damage the microwave oven parts and shorten the life expectancy of the magnetrons. In this paper, we have developed a high-temperature multi-magnetron microwave furnace for high temperature material processing that utilizes magnetrons, high voltage diodes and a high voltage capacitor from a domestic microwave oven. We used Comsol Multi-physics to model the wave propagation in the waveguide and in the cavity to optimize the cavity size, the configurations of waveguides and the door's choke. In this way the electric field intensity is highest at the center of the cavity, there is limited electric field reflection into the waveguide and harmless microwave leakage. The furnace was fabricated and then, experimental verifications of microwave leakage and high temperature heating were done. The development of the furnace is discussed in detail in the following sections.

2. Modeling of Microwave Propagation and Furnace Optimization

In order to design the microwave furnace, the study of microwave propagation by modeling and simulation is indispensable. Comsol Multi-physics software was used to analyze the wave field distributions in the cavity and in the waveguides. Thus the furnace structure, including cavity size, waveguide arrangement, door choke, can be optimized. Modeling and optimization can reduce the cost and time for the development of the furnace (Singh, Gupta, Jain, & Sharma, 2015).

2.1 Modeling procedure

Multi-mode microwave furnaces have four main components; cavity, waveguide, magnetron and door. Radiative microwaves from magnetron is transmitted through the waveguide into the cavity to heat the materials. The microwave propagation in the furnace is modelled by Maxwell's equations with boundary conditions. The wave equation for the electric field and its boundary conditions are given by equations (1) and (2), respectively (COMSOL, 2005).

$$\nabla \times \mu_r^{-1}\left(\nabla \times \vec{E}\right) - k_0^2\left(\varepsilon_r - \frac{j\sigma}{\omega\varepsilon_0}\right) = 0 \quad (1)$$

$$\hat{n} \times \vec{E} = 0 \quad (2)$$

E is the electric field intensity, μ_r is the relative permeability, ε_r is the relative permittivity, ε_0 is the permittivity of free space, σ is the electrical conductivity of the material, k_0 is the propagation constant and ω is the angular frequency and $\hat{n}$ is the unit vector perpendicular to the wall.

The walls of the waveguides and cavity are considered as perfect conductors, therefore the tangential electric field component is zero (COMSOL, 2005). The spatial distribution of the electric field E(r) can be obtained by analytical methods (Griffiths & Schiesser, 2010) or numerical methods (Canale & Chapra, 2014). Because of the asymmetry of the cavity, it is very difficult to solve the equation analytically. Therefore, the solutions of the electric wave equations are approximated using the numerical method (Taflove & Hagness, 2005). Comsol Multi-physics software (Huang, Chen, & Wang, 2015) is used to obtain *E(r)* in this work. Comsol Multi-physics is a powerful software package which includes a numerical solver, geometric tool and visualization. The solver applies the finite element method (FEM) to solve the equations.

2.2 Furnace optimization

For high-temperature material processing, the microwave furnace has to supply enough electric field energy to heat the material samples, placed at the center of the cavity. Moreover, the microwave furnace has to be safe from harmful microwave leakage. In this work, an intense electric field was achieved by combining microwave electric fields from four magnetrons. The configuration of the waveguides must be exact to reduce damage to the magnetrons by leakage of electric waves from opposite waveguides. For effective transmission of microwaves from the waveguides into the cavity, the dimension of the cavity is crucial. Prevention of leakage of the electric field at the door edge was accomplished with an appropriate door choke (Schubert & Regier, 2005). Optimization of the waveguide configuration, cavity's dimension and door choke will be discussed in detail in the following sections.

2.2.1 Waveguide configuration

Figure 1 shows a model of the two-waveguide and two-magnetron configuration. Experimentally, the magnetron was mounted on each waveguide, something not shown in the model. The waveguides, WG1 and WG2, are placed on opposite sides of the cavity.

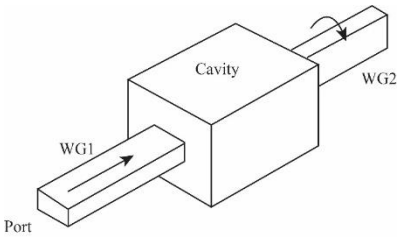

Figure 1. Two-waveguide and two-magnetron model for studying the optimization of the waveguide configuration.

The model was used to study optimization of the waveguide configuration for minimum leakage of the electric field into each other, to prevent the magnetrons from being damaged by self-heating. The relative angle of orientation of the two waveguides was investigated for minimum electric field leakage. In the calculations of the electric field distribution *E(r)* inside the cavity and waveguides, the microwave power was 800 W, at a frequency of 2.45 GHz and TE_{10} mode injected through the port of WG1 for different orientations of WG2. Spatial dependence of the electric field norm $E_{norm} = \mathrm{sqrt}(\vec{E} \cdot \vec{E}^*)$ was obtained for each relative angle. Figure 2 shows the distribution of the electric field inside the cavity and waveguides on the xz-plane and z-axis when the relative angles were 90°. The electric field did not propagate into WG2 when the relative angle was 90°, and there was no leakage of the electric field into WG2 from WG1. Inside WG2, at $z > 20$ cm, the electric field was minimized at about zero, as shown in Figures 2a and 2b. On the other hand, when relative angle was 0 ° the electric field propagated freely into WG2 to form a standing wave at $z > 20$ cm, and maximum leakage of the electric field occurred. Consequently, the two waveguides were mounted on opposite sides of the cavity at 90° relative to each other to minimize electric field leakage.

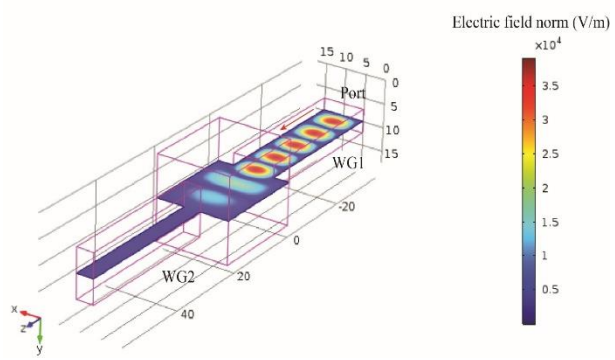

(a)

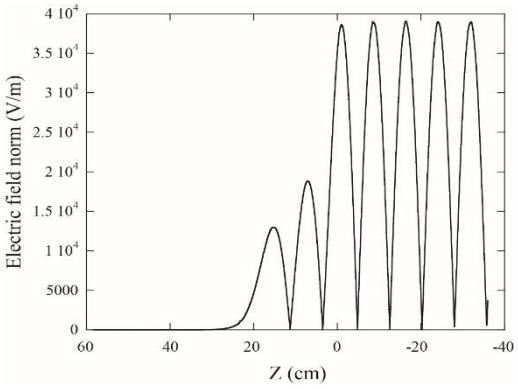

(b)

Figure 2. Distribution of the electric field inside the cavity and waveguides on (a) xz-plane at y = 7.5 cm and (b) z-axis at x = 5 cm and y = 7.5 cm, when the relative angle is 90 ° and the port of WG1 is at z = -40 cm.

The cutoff frequency for TE mode in a rectangular waveguide is determined by equation (3).

$$f_{c,mn} = \frac{1}{2\pi\sqrt{\mu\varepsilon}}\sqrt{\left(\frac{m\pi}{a}\right)^2 + \left(\frac{n\pi}{b}\right)^2} \quad (3)$$

where m , n = 0,1,2,3… ($m \neq n \neq 0$), a is inner width and b is inner height.

The microwave can propagate through this waveguide only when a > b. For WR430 waveguide, the cross section dimensions of WG1 are a = 109.22 mm and b = 54.61 mm. The TE_{10} mode cutoff frequency is 1.372 GHz. On the other hand, the perpendicular opposite waveguide WG2 have a = 54.61 mm and b = 109.22 mm, where a < b. The TE_{10} mode cutoff frequency is 2.64 GHz. Thus, the microwave frequency 2.45 GHz did not propagate from WG1 into WG2 when the relative angle was 90°.

2.2.2 Impedance matching and power combination

Heating of the materials occurred inside the cavity, where the electric field energy was stored. The only loss was due to surface heating of the conductive wall surfaces, which was negligible. The lumped element model of the furnace, including waveguides and cavity, had only LC (Bakshi, 2009) networks. Impedance matching determined the efficiency of

microwave power transmission from the waveguides into the cavity. The impedance of the cavity is a function of its dimension (Mehdizadeh, 2015). Figure 3a shows the model of microwave furnace used for investigation of impedance matching. There were four waveguides mounted to each side wall of the multi-mode rectangular cavity, opposite waveguides were 90° relative to each other, while the cavity dimensions were $L \times L \times L$. In the calculations of $E(r)$, a microwave power of 800 W, a frequency of 2.45 GHz and TE_{10} mode injected simultaneously through the ports of WG1, WG2, WG3 and WG4 were used.

It was found that when L = 28 cm, the field peaked inside the cavity, and was minimized inside the waveguides, as shown in Figures 3b, matching impedance was satisfied and the microwave power was transmitted effectively from the waveguides into the cavity. Therefore, the cavity of the microwave furnace must have dimensions of 28 × 28 × 28 cm^3 for maximum microwave power transmission.

In order to study the combination of microwave power from four magnetrons, $|E|^2$ at the cavity's center was obtained for L = 28 cm. In the model, the magnetrons were represented by ports WG1, WG2, WG3 and WG4, where the microwave power was injected. In the calculation of $|E|^2$, the number of magnetrons was increased one by one, from one to four magnetrons. It was found that $|E|^2$ increased linearly with the number of magnetrons. Since the microwave power was proportional to $|E|^2$, the power could be increased by increasing the number of operational magnetrons, when 4 magnetrons are used, 4 times the power of one magnetron obtained.

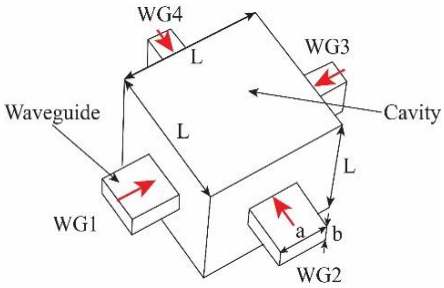

(a)

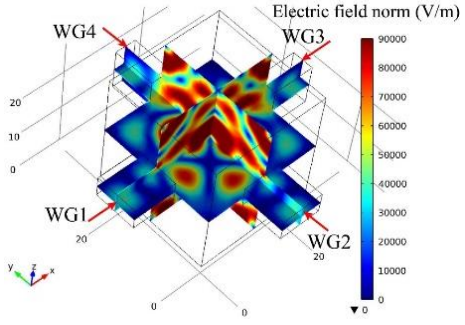

(b)

Figure 3. (a) The model of the microwave furnace, consisting of a multi-mode rectangular cavity and four waveguides mounted to each side wall of the cavity (b) Distributions of the electric field norm inside the waveguides and cavity.

2.2.3 Door choke and leakage suppression

The International Electrotechnical Commission (IEC) (Ong & Akbarnezhad, 2014) has defined the safety standard of microwave leakage to be a leakage power density that does not exceed 5 mW /cm^2 at a distance of 5 cm from the external surface. Because of uneven metal surfaces, microwave leakage occurred at the millimeter-scale door-cavity gap, typically higher than 5 mW/cm^2. This microwave leakage will cause interference with other electrical devices and may be harmful for the living environment. Therefore, the door of the microwave furnace must have chokes (Clemente-Fernandez et al., 2012) for suppression of microwave leakage to reach the safety standard. The choke is periodically cut metal, installed on the edge of the door as shown in Figure 4a. Figure 4b shows the computational model to optimize the shape and dimension of the choke, G is the distance between bar and cavity wall, h is the distance between cavity wall and choke, w is the width of the choke, d is the distance between the bar and choke.

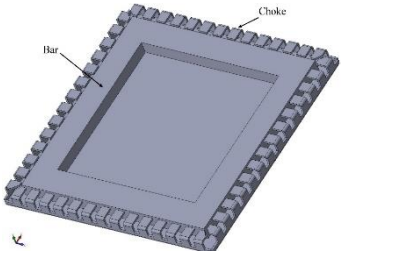

(a)

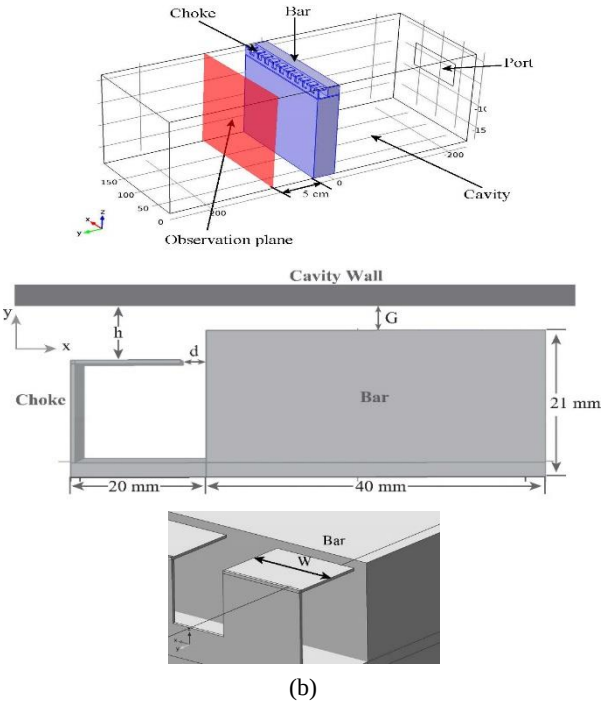

(b)

Figure 4. (a) The microwave furnace door and its choke on the door edge (b) The computational model to optimize the shape and dimension of the choke, G is the distance between bar and cavity wall, h is the distance between the cavity wall and choke, w is the width of the choke, d is the distance between the bar and choke

These parameters determine the resonant effect in reflection of microwaves (M. Mehdizadeh, 2015), so that the choke effectively suppresses microwave leakage. In the calculation, the microwave power was set to 800 W injected simultaneously through ports WG1, WG2, WG3 and WG4, microwave leakage power intensity was obtained for G = 1.50 mm, as parameters d, h, w were varied. Ranges of the parameters where the power density is lower than the safety standard were obtained; 2.7mm < d < 3.7 mm, 0 < h < 7.5 mm, w > 6 mm. Therefore, the dimension of door choke was defined in this range so that an effective microwave leakage suppression can be achieved.

3. Furnace Structure and Characteristics

In this section the furnace structure and its accessories, such as power control system, thermocouple and data logger unit, insulator, and crucible susceptor are explained. The furnace was fabricated according to the modeling and optimization in the previous section. The high performance of the furnace was verified by microwave power measurement, microwave leakage measurement, and measurement of silicon carbide crucible temperature. The specifications of the furnace were then given for maximum microwave power, highest heating temperature of the crucible and maximum microwave leakage suppression.

3.1 Furnace structure and component

Figure 5 shows the structure and components of the furnace. The cavity and door were made of stainless steel, their dimensions were obtained from the optimization. The standard aluminum waveguides were WR430 for lunching TE10 mode. The insulator was commercial ceramic fiber which can sustain a maximum temperature of about 1260 ºC (*ISOLITE B-7 insulation brick*). The drawing and picture of the furnace and its components are shown in Figures 5a and 5b, respectively. The ceramic fiber insulator covers all the inner walls of the cavity to preserve the high temperature. The SiC crucible was put at the center of the cavity where the microwave electric field was highest, as was derived in section 2. The door and its choke was designed to be on the top of the furnace for convenience in loading of the samples and the crucible. During the operation of the magnetrons, forced air flow fans cooled the magnetrons to keep the temperature less than 150 ºC.

3.2 Temperature sensor and data logger

Figure 6 shows a diagram of the experimental set-up to measure the temperature of the crucible in the furnace which includes a temperature sensor and data logger. In this work, a type K thermocouple was used as a sensor to measure the SiC crucible's temperature up to 1260 ºC. The thermocouple was inserted through a hole at the bottom of the furnace to contact the bottom of the crucible.

The analog voltage signals from the thermocouple's output were converted to digital signals using MAX31855. Then, the digital signals were sent to a microcontroller by SPI communication for processing to obtain the crucible's temperature values. Finally, a computer obtained the temperature data from the microcontroller through RS232 for recoding and displaying.

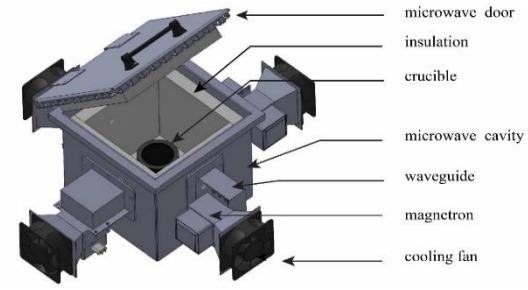

(a)

(b)

Figure 5. (a) Drawing and (b) photograph of the furnace and its components.

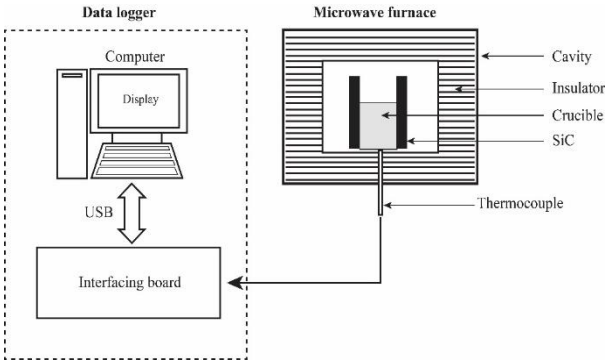

Figure 6. Diagram of the experimental set-up to measure temperature of the crucible in the furnace.

3.3 Microwave power measurement

To verify the calculated results of $|E|^2$ dependence on the number of magnetrons shown in section 2.2.2, microwave powers were measured when a different number of magnetrons were used. Typically, high power microwave in the range of kW can only be measured by calorimetry (Rao, 2012). In this work, 500 cc of water was put at the center of the cavity to absorb microwave energy for 30 s to measure microwave power. The phase angle was fixed at 180° for maximum line input power. The number of magnetrons was increased one by one, from one to four magnetrons. Figure 7 shows that microwave power is clearly proportional to the number of magnetrons for the optimum cavity's dimensions of 28 × 28 × 28 cm^3. The maximum power, when four magnetrons were operated, was about 1,700 W.

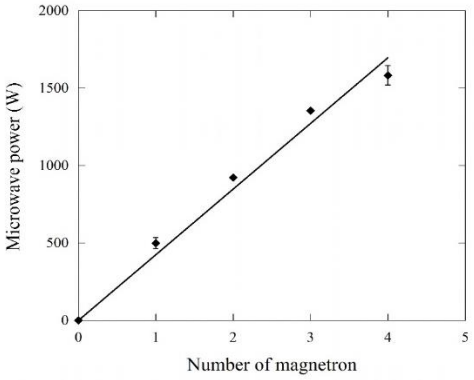

Figure 7. Microwave output power versus number of magnetrons.

3.4 Microwave leakage measurement

The leakage measurement was done with and without the choke. The microwave detector was fixed at 5 cm from the surface of the microwave furnace to measure the microwave leakage for different powers or phase angles. The choke effectively suppressed the leakage to be less than the safety standard of 5 mW/cm^2 as shown in Figure 8. Without the choke the leakage increased slowly with the phase angle. At about 95° the leakage was higher than 5 mw/ cm^2. The results confirm the optimization of the choke's dimensions obtained in section 2.

3.5 Temperature of silicon carbide crucible

To investigate the heating characteristics of the microwave furnace, a SiC crucible was placed at the center of the cavity to absorb microwave energy as shown in Figure 6. Four magnetrons were operated simultaneously at the same phase angle. Figure 9 shows the measurement results of crucible temperatures at each phase angle. The temperatures increased rapidly within a few minutes and then slowly increased with a different slope which increased with phase angle. When the phase angle was 160° the temperature of crucible increased sharply to 900 °C within only 15 minutes, then the increasing rate of the temperature was reduced and took about 30 minutes to reach 1200 ºC. These results show that the temperature of the materials during synthesis can be controlled precisely by varying the phase angles for suitable conditions. Temperature and time are the critical parameters for exploring the synthesis of advanced materials.

3.6 Synthesis of thermoelectric material at high temperature

To verify the advantage of the microwave furnace, the thermoelectric material Aluminum doped Zinc Oxide (Al-doped ZnO) was synthesized by a solid state reaction with heating in the microwave furnace. The sintering time of the Al-doped ZnO sample was compared with the conventional sintering method in an electric furnace. Figure 10 shows that the sintering time by microwave heating is significantly decreased, more than 20 times. The microwave sintering can increase the temperature from room temperature to 1200 °C within only 20 minutes. The Al-doped ZnO samples were tested for their thermoelectric properties to convert heat into electric power. The results show that thermoelectric conversion of the

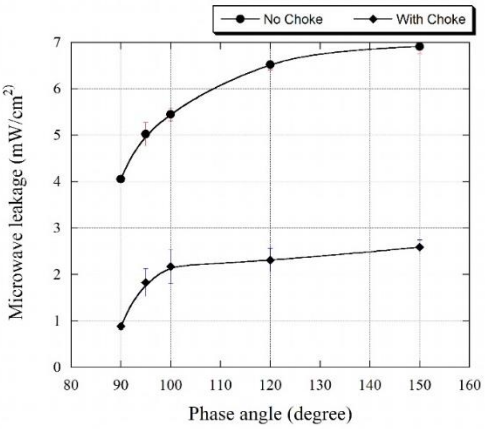

Figure 8. The comparison of the microwave leakage with choke and without choke for each phase angle.

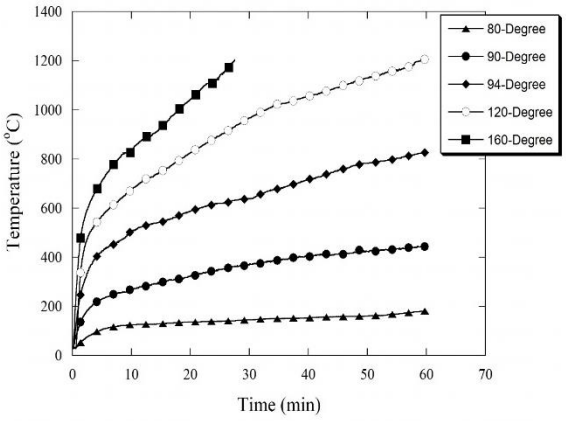

Figure 9. The temperature of the crucible (silicon carbide; SIC) and the phase angle at 80, 90, 93, 94, 120 and 160 °.

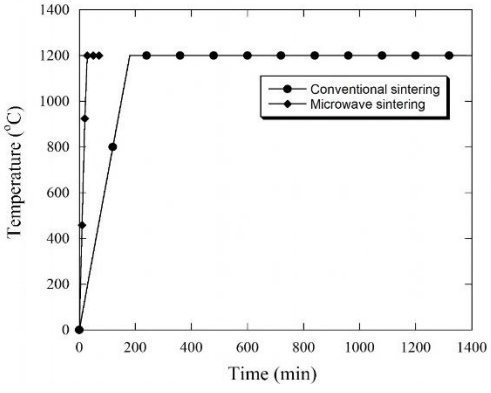

Figure 10. A comparison of heating between the microwave and conventional sintering of Zinc Aluminum Oxide on the sintering time.

Al-doped ZnO by the microwave furnace was a little higher than by the electric furnace. This results were due to the effects of heating rates that control the grain size of the thermoelectric materials (Mishra & Sharma, 2016). The rapid sintering time produced lower average grain sizes that enhance the thermoelectric power (Kadhim, Hmood, & Abu Hassan, 2013).

4. Summary and Conclusion

The numerical simulation and experimental verification was applied for the development of a multi-magnetron microwave furnace for high-temperature material processing. Furnace structure was designed by numerical simulation to optimize their position of waveguide cavity size and dimension of choke. To prevent the magnetrons from self-heating damage, the two waveguides at the opposite side of rectangular cavity were perpendicular position. In case of four waveguide microwave furnace, rectangular cavity size was calculated as $28 \times 28 \times 28$ cm^3 which is matching with maximum microwave power transmission. The highest electric filed intensity was founded at the center of the rectangular cavity. Intensity of electric filed increased by four times when applied four waveguides. It showed linear relation. Choke which is leakage suppression was studied parameters dimensions, 2.7 mm < d < 3.7 mm, 0 < h < 7.5 mm and, w > 6 mm. The dimension of this choke has an advantage in which amount of microwave leaked form the rectangular cavity lower than the standard safety.

The microwave oven magnetrons, electronics and metals, available in the local market were used to fabricate the microwave furnace under simulation conditions. The microwave furnace performance was verified. The microwave power depended on number of magnetron and phase angle. Moreover, the maximum power of microwave furnace was measured as 1700 W. The microwave leakage was lower than 5 mW/cm^2. Microwave furnace can heat SiC crucible rising to 1000 ^oC within only few minutes.

Times for synthesis of Al-doped ZnO to be thermoelectric material by using microwave furnace was dramatically lower than that of conventional furnace by 20 times. The thermoelectric power of Al-doped ZnO synthesized by microwave furnace was higher than that of synthesized by conventional furnace.

In conclusion, a high-temperature microwave furnace was successfully developed. The furnace could synthesize materials effectively, with less time and high quality. Scaling up the microwave furnace for an industrial prototype will be developed in the future.

Acknowledgements

The research work was supported by Walailak University, Thailand. Rajamangala University of Technology Krungthep, Thailand. King Mongkut's Institute of Technology Ladkrabang, Thailand.

References

Bakshi, A. V. (2009). *Transmission lines and waveguide*. Maharashtra, India: Technical Publications.

Bhattacharya, M., & Basak, T. (2016). A review on the susceptor assisted microwave processing of materials. *Energy*, *97*, 306-338. doi:10.1016/j.energy.2015.11.034

Canale, R., & Chapra, S. (2014). *Numerical methods for engineers*. New York, NY: McGraw-Hill Education.

Clemente-Fernandez, F. J., Monzo-Cabrera, J., Catala-Civera, J. M., Pedreno-Molina, J. l., Lozano-Guerrero, A. J., & Diaz-Morcillo, A. (2012). Waveguide bandstop filter based on irises and double corrugations for use in industrial microwave ovens. *Electronics Letters, 48*(13), 772-774. doi:10.1049/el.2012.1211

COMSOL. (2005). *COMSOL Multiphysics: User's guide*. Burlington, MA: COMSOL.

Griffiths, G., & Schiesser, W. E. (2010). *Traveling wave analysis of partial differential equations: Numerical and analytical methods with matlab and maple*. Amsterdam, The Netherlands: Elsevier Science.

Huang, Z., Chen, L., & Wang, S. (2015). Computer simulation of radio frequency selective heating of insects in soybeans. *International Journal of Heat and Mass Transfer*, *90*, 406-417. doi:10.1016/j.ijheatmass transfer.2015.06.071

Kadhim, A., Hmood, A., & Abu Hassan, H. (2013). Thermoelectric generation device based on p-type Bi0.4Sb1.6Te3 and n-type Bi2Se0.6Te2.4 bulk materials prepared by solid state microwave synthesis. *Solid State Communications, 166*, 44-49. doi:10.1016/j.ssc.2013.04.020

Mehdizadeh, M. (2015). *Microwave/RF applicators and probes* (2nd Ed.). Chapter 5 - Microwave multimode cavities for material heating (pp. 153-183). Boston, MA: William Andrew Publishing.

Mehdizadeh, M. (2015). *Microwave/RF applicators and probes: for material heating, sensing, and plasma generation*. Amsterdam, The Netherlands: Elsevier Science.

Mishra, R. R., & Sharma, A. K. (2016). Microwave–material interaction phenomena: Heating mechanisms, challenges and opportunities in material processing. *Composites Part A: Applied Science and Manufacturing, 81*, 78-97. doi:10.1016/j.compositesa.2015.10.035

Oghbaei, M., & Mirzaee, O. (2010). Microwave versus conventional sintering: A review of fundamentals, advantages and applications. *Journal of Alloys and Compounds, 494*(1–2), 175-189. doi:10.1016/j.jallcom.2010.01.068

Ong, K. C. G., & Akbarnezhad, A. (2014). *Microwave-Assisted concrete technology: production, demolition and recycling*. Oxfordshire, England: Taylor and Francis.

Panneerselvam, M., Agrawal, A., & Rao, K. J. (2003). Microwave sintering of MoSi2–SiC composites. *Materials Science and Engineering: A, 356*(1–2), 267-273. doi:10.1016/S0921-5093(03)00140-0

RAO, R. S. (2012). *Microwave Engineering* (pp. 470-480). New Delhi, India: PHI Learning.

Schubert, H., & Regier, M. (2005). *The microwave processing of foods*: Oxfordshire, England: Taylor and Francis.

Singh, S., Gupta, D., Jain, V., & Sharma, A. K. (2015). Microwave processing of materials and applications in manufacturing industries: A review. *Materials and Manufacturing Processes, 30*(1), 1-29. doi:10.1080/10426914.2014.952028

Taflove, A., & Hagness, S. C. (2005). *Computational electrodynamics: The Finite-difference Time-domain Method*. Norwood, MA: Artech House.